

6-2018

Elementary Computational Fluid Dynamics Using Finite-Difference Methods

Jason Turner

Union College - Schenectady, NY

Scott LaBrake

Union College - Schenectady, NY

Follow this and additional works at: <https://digitalworks.union.edu/theses>



Part of the [Fluid Dynamics Commons](#)

Recommended Citation

Turner, Jason and LaBrake, Scott, "Elementary Computational Fluid Dynamics Using Finite-Difference Methods" (2018). *Honors Theses*. 1581.

<https://digitalworks.union.edu/theses/1581>

This Open Access is brought to you for free and open access by the Student Work at Union | Digital Works. It has been accepted for inclusion in Honors Theses by an authorized administrator of Union | Digital Works. For more information, please contact digitalworks@union.edu.

Elementary Computational Fluid Dynamics Using Finite-Difference Methods

By

Jason Turner

* * * * *

Submitted in partial fulfillment
of the requirements for
Honors in the Department of Physics and Astronomy

UNION COLLEGE

June 2018

ABSTRACT

TURNER, JASON Elementary Computational Fluid Dynamics Using Finite-Difference
Methods. Department of Physics and Astronomy, June 2018.

ADVISOR: LaBrake, Scott

Fluids permeate all of human existence, and fluid dynamics serves as a rich field of research for many physicists. Although the mathematics involved in studying fluids tends to get complicated, the physical intuition gained through daily exposure to such systems bridges the gap between abstract calculations and their physical meaning. We discuss the mathematical treatment and simulations of fluid flows found in everyday life, such as flow in a cavity and through a pipe. Our discussions follow the example set by several notable texts, such as [1], [3], [4], and [5].

Contents

Chapter 1	Introduction	1
1.1	Elementary Ideal Flows	3
Chapter 2	Viscous Fluid Flows	11
2.1	Examples of Elementary Viscous Flows	12
Chapter 3	The Finite-Difference Method and the Navier-Stokes Equation	15
3.1	First-Order Derivatives	15
3.2	Poisson's Equation and Second-Order Derivatives	17
3.3	The Navier-Stokes Equations	19
3.4	Implementation Examples	22
3.4.1	Cavity Flow	22
3.4.2	Channel Flow	24
3.4.3	Channel Flow with Blockage	25

Chapter 1: Introduction

The study of fluid mechanics dates back to the ancient Greeks, who introduced ideas such as Archimedes' Principle¹ and elementary hydraulic machinery. It continues to be a highly active research area, featuring many popular subfields including:

- Astrophysical fluids, including galaxies and stars;
- Geophysical fluids, including the earth's atmosphere and oceans;
- Biological fluids, including blood, and;
- Aerodynamics, including airplanes and other aircraft.

Fluids consist of a very large number of individual molecules, whose motion we cannot easily calculate. For instance, 18 grams of water contains approximately 6.022×10^{23} molecules, each of which undergoes various accelerations as the fluid flows. However, many practical applications of fluid mechanics are on length scales much longer than the typical intermolecular spacing.

Hence, in our study of fluids, we “smooth out” the molecular details by assigning the velocity of a fluid at a point \mathbf{x} and time t to be the average velocity in a fluid element δV centered on \mathbf{x} at time t . We define the velocity field $\mathbf{u}(\mathbf{x}, t)$ of the fluid as a smooth function. We similarly define the density of a fluid at a point \mathbf{x} and time t as the quotient of the mass contained in a volume element δV and the volume element δV . This is known as the **continuum hypothesis**.

¹Archimedes' Principle states that the force of buoyancy an object experiences is equal to the weight of fluid it displaces. This is different than the infamous tale of his “eureka” moment, in which he realized that the volume of displaced fluid is equal to the volume of the submerged object.

In addition to the continuum hypothesis, we limit our study to fluids and flows with the following properties:

- i. **Isotropic**: There are no preferred directions in a fluid.
- ii. **Newtonian**: There is a linear relationship between the local shear stress and the local rate of strain, as well as between the local heat flux density and the local temperature gradient.
- iii. **Classical**: The flow is well-described by Newtonian mechanics, and both quantum and relativistic effects may be ignored.
- iv. **Incompressible**: A given fluid element maintains its volume as it moves. This is expressed by the **incompressibility condition**

$$\nabla \cdot \mathbf{u} = 0. \quad (1.1)$$

A fluid is said to be **ideal** if, in addition to (i) – (iv), we have

- v. **Inviscid**: Each fluid element does not exert a stress on nearby fluid elements. In other words, the force exerted across a surface element $\hat{\mathbf{n}} \delta S$ within the fluid is

$$p \hat{\mathbf{n}} \delta S,$$

where $p(\mathbf{x}, t)$ is a scalar function independent of the normal $\hat{\mathbf{n}}$, called the **pressure**. Using Stokes' Theorem, we find that the net force exerted on a volume of fluid V enclosed in a surface S by the surrounding fluid is

$$-\int_S p \hat{\mathbf{n}} dS = -\int_V \nabla p dV.$$

Hence, the net force on δV due to the pressure of the surrounding fluid is $-\nabla p \delta V$.

Although not every fluid we study will be ideal, they will have properties (i) – (iv).

Section 1.1: Elementary Ideal Flows

Through studying ideal flows, one is able to cross the frontier into studying fluid dynamics without the burden of considering more complicated properties of real-world fluids, such as compressibility and viscosity. We begin by defining some special classes of flows with simplifying features, and then introduce several useful geometric and mathematical tools for studying them. We describe flow velocity as a vector $\mathbf{u} = \langle u, v, w \rangle$ dependent on position $\mathbf{x} = \langle x, y, z \rangle$ and time t .

A **steady flow** is one which is not dependent on time, i.e.,

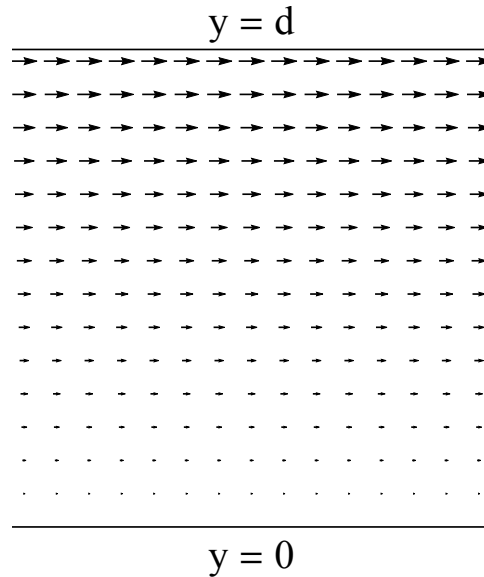
$$\frac{\partial \mathbf{u}}{\partial t} = \mathbf{0}. \quad (1.2)$$

This implies that, at any fixed point in space, the speed and direction of flow are constant.

Example 1.1. Consider the steady flow defined by

$$u = U y, \quad v, w = 0,$$

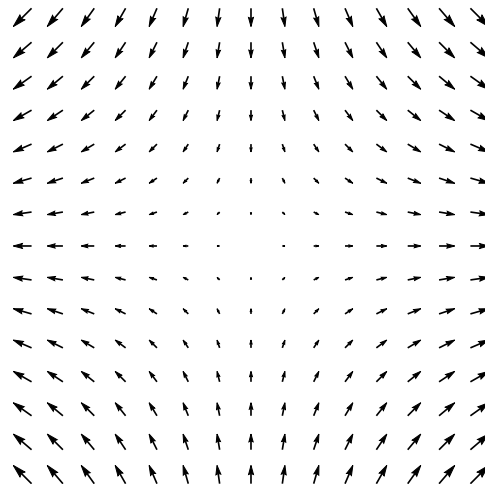
for some positive constant U (with units of inverse time) and y is the vertical height in the fluid (shown in Figure 1.1). This is known as a *shear flow*, as adjacent layers of fluids move parallel to each other with different speeds. Real-world examples of shear flow include wind blowing across a lake and water flowing down a stream. As both U and y are constant with respect to time, this flow is steady.

Figure 1.1: A *shear flow* with $U = 0.1$.

Example 1.2. A *stagnation-point flow* is one for which $\mathbf{u} = \mathbf{0}$ at some point \mathbf{x} . For instance, the flow defined by

$$u = Ux, \quad v = -Uy, \quad w = 0$$

has a *stagnation point* located at the origin, as shown in the figure below. Water flowing vertically outward from a small fountain is an example of a stagnation-point flow.

Figure 1.2: A *stagnation-point flow* with $U = 0.1$, featuring a *stagnation point* at the origin.

A **two-dimensional flow** is one which is independent of some spatial coordinate. It follows

that a **steady two-dimensional flow** is independent of both some spatial coordinate and time (see Example 1.2). In reality, no flow can be truly two-dimensional, although there are cases where such a simplification is valid, such as flow down a pipe.

When studying fluid flow, one may wish to create neat geometric objects which “match” the flow velocity at various points. The concept of **streamlines** accomplishes this task handily; they are curves which have the same direction as the fluid flow $\mathbf{u}(\mathbf{x}, t)$ at every point at a specific moment in time. A streamline $(x(s), y(s), z(s))$ parametrized by the variable s satisfies the equation

$$\frac{dx/ds}{u} = \frac{dy/ds}{v} = \frac{dz/ds}{w}, \quad (1.3)$$

at a particular time t .

Example 1.3. Recall the stagnation-point flow defined in Example 1.2:

$$u = Ux, \quad v = -Uy, \quad w = 0.$$

By solving the differential equation

$$\frac{dx}{Ux} = -\frac{dy}{Uy},$$

we may find that the streamlines of the flow are of the form

$$y = \frac{a}{x}$$

for some real constant a , and can be seen in Figure 1.3.

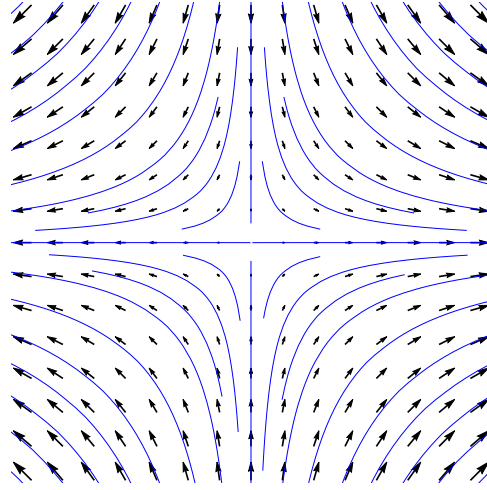


Figure 1.3: *The streamlines of a stagnation-point flow with $U = 0.1$, featuring a stagnation point at the origin.*

From this idea, the question of how properties of the fluid change along streamlines naturally arises. We denote a given property of interest as $f(\mathbf{x}, t)$, which may be a component of flow velocity \mathbf{u} or density ρ . The partial derivative $\partial f / \partial t$ denotes the rate of change of f with respect to time at a fixed position. In contrast, the rate of change of f following the fluid, denoted Df / Dt , is

$$\frac{Df}{Dt} = \frac{d}{dt} f(x(t), y(t), z(t), t)$$

where $x(t)$, $y(t)$, and $z(t)$ are understood to change with time at the local flow velocity \mathbf{u}

$$\frac{dx}{dt} = u, \quad \frac{dy}{dt} = v, \quad \frac{dz}{dt} = w.$$

Through applying the chain rule, we obtain

$$\begin{aligned} \frac{Df}{Dt} &= \frac{d}{dt} f(x(t), y(t), z(t), t) \\ &= \frac{\partial f}{\partial t} + u \frac{\partial f}{\partial x} + v \frac{\partial f}{\partial y} + w \frac{\partial f}{\partial z} \\ &= \frac{\partial f}{\partial t} + (\mathbf{u} \cdot \nabla) f. \end{aligned} \tag{1.4}$$

Hence, the acceleration of a fluid element at \mathbf{x} is

$$\frac{D\mathbf{u}}{Dt} = \frac{\partial \mathbf{u}}{\partial t} + (\mathbf{u} \cdot \nabla) \mathbf{u}. \quad (1.5)$$

In any steady flow, the rate of change of f following a fluid element is $(\mathbf{u} \cdot \nabla) f$. To see this, let \mathbf{e}_s be the unit vector which always points in the direction of the streamlines. It follows that

$$\mathbf{u} \cdot \nabla f = |\mathbf{u}| \mathbf{e}_s \cdot \nabla f = |\mathbf{u}| \frac{\partial f}{\partial s},$$

where s denotes the distance along the streamline.

Example 1.4. Let the concentration of some pollutant in the fluid be

$$c(x, y, t) = \beta x^2 y e^{-U t},$$

for $y > 0$, where β is a constant, and let \mathbf{u} be the stagnation-point flow defined in Example 1.2. One natural question is if the pollutant concentration for any particular fluid element changes with time? To see whether it does or not, we calculate the following derivative:

$$\begin{aligned} \frac{Dc}{Dt} &= \frac{\partial c}{\partial t} + (\mathbf{u} \cdot \nabla) c \\ &= -U \beta x^2 y e^{-U t} + \left(U x \frac{\partial}{\partial x} - U y \frac{\partial}{\partial y} \right) \beta x^2 y e^{-U t} \\ &= -U \beta x^2 y e^{-U t} + 2 U \beta x^2 y e^{-U t} - U \beta x^2 y e^{-U t} = 0. \end{aligned}$$

As this derivative is zero, we see that the concentration of pollutant in a given fluid element is constant with time.

The equation $(\mathbf{u} \cdot \nabla) f = 0$ implies that f is constant along a streamline, although it offers no information about its value elsewhere. Likewise, $Df/Dt = 0$ implies f is constant for a particular fluid element.

With this in mind, we are ready to derive **Euler's equations of motion**, which are the basic

equations of motion for an ideal fluid. Recall from the definition of an inviscid flow that the net force on a fluid element of volume δV is $-\nabla p \delta V$. Including a gravitational body force per unit mass \mathbf{g} , the total force on the element is

$$(-\nabla p + \rho \mathbf{g}) \delta V.$$

From Newton's Second Law, we know that this force must be equal to the product of the volume element's mass (which is conserved due to an ideal fluid's incompressibility) and its acceleration,

$$\rho \delta V \frac{D\mathbf{u}}{Dt}.$$

We thus obtain Euler's equations of motion:

$$\frac{D\mathbf{u}}{Dt} = -\frac{1}{\rho} \nabla p + \mathbf{g}, \quad (1.6)$$

$$\nabla \cdot \mathbf{u} = 0.$$

Example 1.5. A *Rankine vortex*, defined as

$$u_\theta = \begin{cases} \Omega r & r \leq a, \\ \frac{\Omega a^2}{r} & r > a, \end{cases}$$

$$u_r = u_z = 0,$$

where Ω is a real constant, is commonly used as a simple model of real vortices, such as whirlpools and tornadoes. The pressure at the center of both of these real-world systems is notably lower than the pressure elsewhere. Using Euler's equations in cylindrical coordinates, we may find the difference in pressure both inside and outside of the core of the Rankine vortex, and compare its behavior to the real-world equivalents.

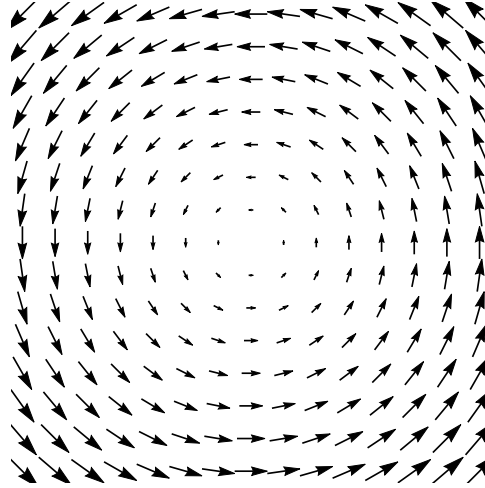


Figure 1.4: The “core” or a Rankine vortex, i.e., the region $r \leq a$.

Note the following identities for cylindrical coordinates:

$$\frac{\partial \hat{\mathbf{e}}_r}{\partial \theta} = \hat{\mathbf{e}}_\theta, \quad \frac{\partial \hat{\mathbf{e}}_\theta}{\partial \theta} = -\hat{\mathbf{e}}_r, \quad \frac{\partial \hat{\mathbf{e}}_z}{\partial \theta} = \mathbf{0},$$

$$\begin{aligned} \nabla p &= \frac{\partial p}{\partial r} \hat{\mathbf{e}}_r + \frac{1}{r} \frac{\partial p}{\partial \theta} \hat{\mathbf{e}}_\theta + \frac{\partial p}{\partial z} \hat{\mathbf{e}}_z, \\ \mathbf{u} \cdot \nabla &= u_r \frac{\partial}{\partial r} + \frac{u_\theta}{r} \frac{\partial}{\partial \theta} + u_z \frac{\partial}{\partial z}. \end{aligned}$$

Using these alongside Euler’s equations, we obtain

$$-\frac{1}{\rho} \left(\frac{\partial p}{\partial r} \hat{\mathbf{e}}_r + \frac{1}{r} \frac{\partial p}{\partial \theta} \hat{\mathbf{e}}_\theta + \frac{\partial p}{\partial z} \hat{\mathbf{e}}_z \right) - g \hat{\mathbf{e}}_z = -\frac{u_\theta^2}{r} \hat{\mathbf{e}}_r$$

keeping in mind that $u_r = u_z = 0$ and $\partial u_\theta / \partial \theta = 0$ for both $r < a$ and $r > a$.

In the case that $r < a$, $u_\theta = \Omega r$ and we obtain the following two equations:

$$-\frac{1}{\rho} \frac{\partial p}{\partial r} = -\Omega^2 r, \quad -\frac{1}{\rho} \frac{\partial p}{\partial z} - g = 0$$

By integrating these two equations, we find that

$$p_{r<a}(r) = \frac{1}{2} \Omega^2 r^2 \rho - g z \rho + c_1$$

which notably attains a value of $-g z \rho + c_1$ at $r = 0$ and $\frac{1}{2} \Omega^2 a^2 \rho - g z \rho + c_1$ at $r = a$.

In the case that $r > a$, $u_\theta = \frac{\Omega a^2}{r}$ and we obtain the following equations:

$$-\frac{1}{\rho} \frac{\partial p}{\partial r} = -\frac{\Omega^2 a^4}{r^3}, \quad -\frac{1}{\rho} \frac{\partial p}{\partial z} - g = 0$$

By integrating these two equations, we find that

$$p_{r>a}(r) = -\frac{\Omega^2 a^4 \rho}{2 r^2} - g z \rho + c_2$$

which notably approaches $-g z \rho + c_2$ as $r \rightarrow \infty$ and attains the value $-\frac{1}{2} \Omega^2 a^2 \rho - g z \rho + c_2$ at $r = a$.

By continuity of the pressure in the fluid, $p_{r<a}(a) = p_{r>a}(a)$, and thus $c_2 - c_1 = \Omega^2 a^2 \rho$. This is also the difference in pressure at $r = 0$ and as $r \rightarrow \infty$. Hence, the pressure is lower at the center of the Rankine vortex.

Elementary ideal flows serve as a sufficient introduction to the theoretical study of fluid flows. They are, however, fundamentally different than viscous flows; the behavior of a fluid as its viscosity approaches 0 is completely unlike an inviscid flow. For this reason, we must consider viscosity if we are to apply our ideas to real-world flows.

Chapter 2: Viscous Fluid Flows

In contrast to inviscid fluids, in a **viscous fluid** each fluid element may exert a force on all nearby elements, referred to as the stresses within the fluid. For example, consider the shear flow $\mathbf{u} = \langle u(y), 0, 0 \rangle$. The tangent component of the stress in this flow τ , which is the component perpendicular to a fluid element surface, is typically zero for inviscid fluids. As we are dealing instead with a viscous Newtonian fluid, there is a linear relationship between the local shear stress and the local rate of strain

$$\tau = \mu \frac{du}{dy} \quad (2.1)$$

where μ is the **coefficient of viscosity** of the fluid.

Of greater interest is the **kinematic viscosity** of the fluid, which is given by

$$\nu = \frac{\mu}{\rho}. \quad (2.2)$$

Throughout our studies, we concentrate on a simple model of fluid flow in which μ , ρ , and ν are all constant.

This ability to exert stress extends to fluid flowing along a boundary, resulting in a boundary layer present between the bulk fluid and said boundary. In fact, at a rigid boundary, both the normal and tangential components of fluid velocity must be equal to those of the boundary itself. This is called the **no-slip condition**, which holds for a fluid of any viscosity, despite how small. It is one of the many reasons that the behavior of a fluid of low viscosity may be

completely different to that of an inviscid fluid.

To account for viscosity, we must add an additional term to the Euler equations

$$\frac{\partial \mathbf{u}}{\partial t} + (\mathbf{u} \cdot \nabla) \mathbf{u} = -\frac{1}{\rho} \nabla p + \nu \nabla^2 \mathbf{u} + \mathbf{g}, \quad (2.3)$$

$$\nabla \cdot \mathbf{u} = 0.$$

These are known as the **Navier-Stokes equations** for an isotropic, Newtonian, classical, incompressible fluid of constant density ρ and constant viscosity ν .

Section 2.1: Examples of Elementary Viscous Flows

Example 2.1. Consider a viscous fluid flowing between two stationary rigid boundaries located at $y = \pm h$ under a constant a pressure gradient $P = -dp/dx$. Due to the constant pressure gradient, the fluid must flow entirely in the \hat{x} direction. If the flow speed were dependent on x , the pressure gradient would not be constant, as the pressure would fluctuate with flow velocity throughout the fluid. A similar argument may be made for any possible dependence on z and t .

Thus, the flow velocity is of the form $\mathbf{u} = \langle u(y), 0, 0 \rangle$, and we simplify the Navier-Stokes equations to

$$-\frac{1}{\rho} \frac{dp}{dx} + \nu \frac{\partial^2 u}{\partial y^2} = 0,$$

$$\nabla \cdot \mathbf{u} = 0.$$

We may rearrange this equation to obtain

$$\frac{\partial^2 u}{\partial y^2} = -\frac{P}{\rho \nu},$$

and integrate twice to obtain

$$u(y) = -\frac{P y^2}{2 \mu} + C_1 y + C_2,$$

where C_1 and C_2 are constants of integration. The no-slip condition implies $u(-h) = u(h) = 0$. Hence, we obtain

$$\begin{aligned} 0 &= -\frac{P h^2}{2\mu} + C_1 h + C_2, \\ 0 &= -\frac{P h^2}{2\mu} - C_1 h + C_2, \end{aligned}$$

which we may add and subtract cleverly to obtain $C_1 = 0$ and $C_2 = \frac{P h^2}{2\mu}$. Hence,

$$u(y) = \frac{P}{2\mu} (h^2 - y^2).$$

Example 2.2. Consider a viscous fluid flowing down a pipe of circular cross-section $r = a$ under a constant pressure gradient $P = -dp/dz$, where the z -axis is the axis of the pipe. In a similar argument to the previous example, $u_r = u_\theta = 0$ and we obtain a reduced form of the Navier-Stokes equations in cylindrical coordinates

$$\frac{1}{r} \frac{d}{dr} \left(r \frac{du_z}{dr} \right) = -\frac{P}{\mu}, \quad (2.4)$$

$$\nabla \cdot \mathbf{u} = 0, \quad (2.5)$$

with $u_z = u_z(r)$ and boundary conditions $u_z(a) = 0$ and $u_z(0) < \infty$ from the no-slip condition and physical constraints of containment in a pipe, respectively.

By rearranging and integrating the Equation 2.4, we obtain

$$u_z(r) = -\frac{P r^2}{4\mu} + C_1 \log r + C_2,$$

where C_1 and C_2 are constants of integration. By applying the boundary conditions, we find that $C_1 = 0$ and $C_2 = \frac{P a^2}{4\mu}$. Thus, we obtain

$$u_z(r) = \frac{P}{4\mu} (a^2 - r^2).$$

The methods of analysis we have discussed may only “go so far”, as we have heavily relied on symmetries within our system and have restricted the range of flows we have study to those which have analytic solutions to the Navier-Stokes equations. By using numerical methods to approximate fluid flows, we are able to study more complicated and even chaotic phenomena, such as turbulence.

Chapter 3: The Finite-Difference Method and the Navier-Stokes Equation

The finite difference method is a numerical method for solving differential equations by approximating them with difference equations. They serve as one of the most dominant approaches to numerical solutions of partial differential equations, and are particularly easy to implement. We resort to numerical method approximations for complicated fluid flows with no clear analytic solution, which are common in the study of aerodynamics and turbulence.

Sections 3.1 - 3.3 describe how we discretize first- and second-order derivatives, and using those to discretize the Navier-Stokes equations for use in programming. Section 3.4 includes examples of some elementary simulations.

Section 3.1: First-Order Derivatives

In order to guide our discussion on approximating first-order derivatives using finite difference methods, we will implement the method to simulate the 1-D linear convection equation

$$\frac{\partial u}{\partial t} + c \frac{\partial u}{\partial x} = 0. \quad (3.1)$$

Given initial conditions of a system u , Equation 3.1 describes the propagation of the system with speed c without change of shape. This equation is one of the simplest in all of computational fluid dynamics, and may be derived from the Navier-stokes equation by only keeping

the accumulation and convection terms for the x -component of the fluid velocity.

As mentioned previously, the finite difference method is centered on the idea of a secant-line approximation of the derivative (see Figure 3.1), i.e., we use a difference approximation in place of actual derivatives.

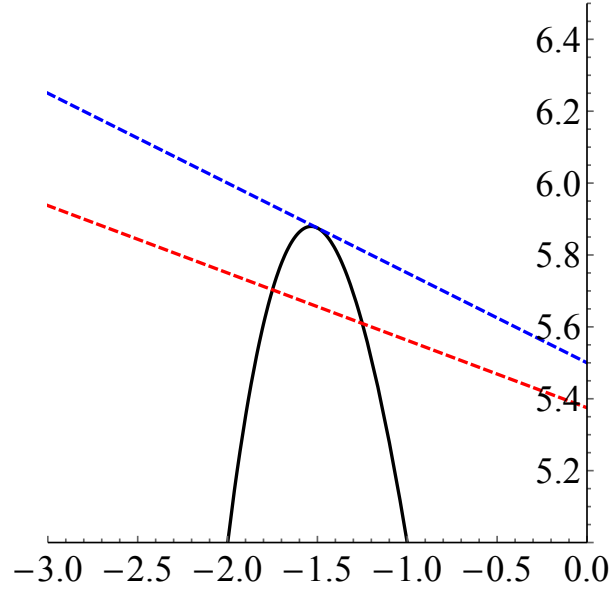


Figure 3.1: A secant-line approximation (red, dashed) of the line (blue, dashed) tangent to $x^3 + x^2 - x + 4$ at $x = -1.5$.

Assume that we know the value of some function $f = f(x)$ at a point x_0 , and we wish to approximate its value at some other x value, say $x_0 + \Delta x$. From the Taylor series of f at x_0 , we obtain

$$f(x_0 + \Delta x) = f(x_0) + \Delta x \left. \frac{df}{dx} \right|_{x_0} + \mathcal{O}(\Delta x^2),$$

where $\mathcal{O}(\Delta x^2)$ denotes a term of order Δx^2 . By rearranging this equation and assuming the error term $\mathcal{O}(\Delta x^2)$ is small, we obtain an approximation for the derivative

$$\left. \frac{df}{dx} \right|_{x_0} \approx \frac{f(x_0 + \Delta x) - f(x_0)}{\Delta x}.$$

This is sometimes referred to as a forward-difference scheme, as we use information about

the point x_0 to gather information about a further point $x_0 + \Delta x$. We may instead consider the x -coordinate as a linear spatial grid, in which the first point is $x_0 = x_0$, the second point is $x_1 = x_0 + \Delta x$, and the i^{th} point is $x_i = x_0 + i \Delta x$.

When applying this approximation to Equation 3.1, we must also introduce a temporal grid in which the first point is t_0 and the n^{th} point is $t_n = t_0 + n \Delta t$ for some fixed temporal spacing Δt . Hence, we may rewrite the 1-D linear convection equation as

$$\frac{u_i^{n+1} - u_i^n}{\Delta t} + c \frac{u_i^n - u_{i-1}^n}{\Delta x} = 0,$$

where n and $n + 1$ in the superscripts are two consecutive steps in time while i and $i - 1$ in the subscripts are neighboring points of the discretized spatial coordinate x . Note that we have used a forward-difference scheme for the temporal derivative and a backward-difference scheme for the spatial derivative (in which we use information about a previous time t_{i-1} to approximate information about the current time t_i). By rearranging this equation, we obtain

$$u_i^{n+1} = u_i^n - c \frac{\Delta t}{\Delta x} (u_i^n - u_{i-1}^n). \quad (3.2)$$

If we are given initial conditions u_i^n for all i , then the only unknown value in this equation is u_i^{n+1} , as c is determined by the system while Δt and Δx are chosen based on the desired accuracy of the approximation.

Section 3.2: Poisson's Equation and Second-Order Derivatives

Poisson's equation, in a similar vein to the 1-D linear convection equation, describes typical diffusion phenomena and is given by

$$\frac{\partial^2 p}{\partial x^2} + \frac{\partial^2 p}{\partial y^2} = b \quad (3.3)$$

where p is a scalar function such as pressure, and b is a “source” term, or an initial distribution of p . For our purposes, using Poisson’s equation for the pressure p of our fluid flow allows us to “smooth out” sharp peaks and discontinuities that may arise from turbulence or trailing edges.

We begin by discretizing second-order derivatives using Taylor series using a central-difference scheme, i.e., using information from x_{i+1} and x_{i-1} to approximate the value of p at x_i . First, consider the Taylor expansions of p_{i+1} and p_{i-1} about p_i with respect to x :

$$\begin{aligned} u_{i+1} &= u_i + \Delta x \left. \frac{\partial u}{\partial x} \right|_i + \frac{\Delta x^2}{2} \left. \frac{\partial^2 u}{\partial x^2} \right|_i + \frac{\Delta x^3}{6} \left. \frac{\partial^3 u}{\partial x^3} \right|_i + \mathcal{O}(\Delta x^4), \\ u_{i-1} &= u_i - \Delta x \left. \frac{\partial u}{\partial x} \right|_i + \frac{\Delta x^2}{2} \left. \frac{\partial^2 u}{\partial x^2} \right|_i - \frac{\Delta x^3}{6} \left. \frac{\partial^3 u}{\partial x^3} \right|_i + \mathcal{O}(\Delta x^4). \end{aligned}$$

By adding these two expansions, we find that

$$u_{i+1} + u_{i-1} = 2u_i + \Delta x^2 \left. \frac{\partial^2 u}{\partial x^2} \right|_i + \mathcal{O}(\Delta x^4),$$

which we may rearrange, assuming $\mathcal{O}(\Delta x^4)$ is small, to obtain

$$\frac{\partial^2 u}{\partial x^2} \approx \frac{u_{i+1} - 2u_i + u_{i-1}}{\Delta x^2}.$$

Using this approximation for Equation 3.3, we obtain

$$\frac{p_{i+1,j}^n - 2p_{i,j}^n + p_{i-1,j}^n}{\Delta x^2} + \frac{p_{i,j+1}^n - 2p_{i,j}^n + p_{i,j-1}^n}{\Delta y^2} = b_{i,j}^n,$$

where n corresponds to the temporal grid, i corresponds to the x -spatial grid, and j corresponds to the y -spatial grid. Rearranging this equation, we obtain

$$p_{i,j}^n = \frac{\left(p_{i+1,j}^n + p_{i-1,j}^n\right) \Delta y^2 + \left(p_{i,j+1}^n + p_{i,j-1}^n\right) \Delta x^2 + b_{i,j}^n \Delta x^2 \Delta y^2}{2 \left(\Delta x^2 + \Delta y^2\right)}. \quad (3.4)$$

Note that there are no terms in this equation of future temporal steps, specifically that it only gives information about p at time step n . We may, however, step through “psuedotime” by recursively iterating this approximation using known information. For instance, assume the source term b consists of two discrete spike and $p = 0$ everywhere initially. After the first use of this approximation, p will be non-zero in the immediate vicinity of the spikes. We may then use the constant source term along with the new distribution of p to obtain a “smoother” approximation of p (see Figure).

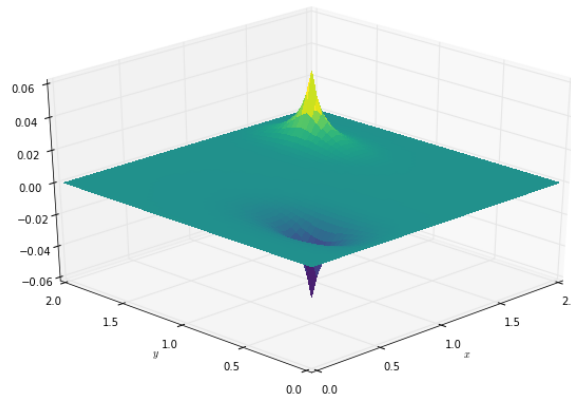


Figure 3.2: Using the finite-difference method, we are able to smooth out the two initial spikes in a source term $b = 100$ at $(1.75, 1.75)$, $b = -100$ at $(0.75, 0.75)$, and $b = 0$ everywhere else.

Section 3.3: The Navier-Stokes Equations

We are now ready to simulate fluid flows using a finite difference approximation of the Navier-Stokes equations. Recall the Navier-Stokes equations (Equation 2.3):

$$\frac{\partial \mathbf{u}}{\partial t} + (\mathbf{u} \cdot \nabla) \mathbf{u} = -\frac{1}{\rho} \nabla p + \nu \nabla^2 \mathbf{u}, \quad (3.5)$$

$$\nabla \cdot \mathbf{u} = 0, \quad (3.6)$$

where we are now ignoring gravity for simplicity (its inclusion would constitute a constant term in Equation 3.5). We may rewrite these equations as

$$\begin{aligned}
\frac{\partial u}{\partial t} + u \frac{\partial u}{\partial x} + v \frac{\partial u}{\partial y} &= -\frac{1}{\rho} \frac{\partial p}{\partial x} + \nu \left(\frac{\partial^2 u}{\partial x^2} + \frac{\partial^2 u}{\partial y^2} \right), \\
\frac{\partial v}{\partial t} + u \frac{\partial v}{\partial x} + v \frac{\partial v}{\partial y} &= -\frac{1}{\rho} \frac{\partial p}{\partial y} + \nu \left(\frac{\partial^2 v}{\partial x^2} + \frac{\partial^2 v}{\partial y^2} \right), \\
\frac{\partial u}{\partial x} + \frac{\partial v}{\partial y} &= 0.
\end{aligned}$$

There is a slight complication when immediately using these equations to simulate fluid flow; each equation has coupled pressure and flow velocity, which we need to approximate separately. To amend this, we take a spatial derivative of the first two equations

$$\begin{aligned}
\frac{\partial}{\partial t} \left[\frac{\partial u}{\partial x} \right] + u \frac{\partial^2 u}{\partial x^2} + \left(\frac{\partial u}{\partial x} \right)^2 + v \frac{\partial^2 u}{\partial x \partial y} + \frac{\partial v}{\partial x} \frac{\partial u}{\partial y} &= -\frac{1}{\rho} \frac{\partial^2 p}{\partial x^2} + \nu \left(\frac{\partial^3 u}{\partial x^3} + \frac{\partial^3 u}{\partial x \partial y^2} \right), \\
\frac{\partial}{\partial t} \left[\frac{\partial v}{\partial y} \right] + u \frac{\partial^2 v}{\partial y \partial x} + \frac{\partial u}{\partial y} \frac{\partial v}{\partial x} + v \frac{\partial^2 v}{\partial y^2} + \left(\frac{\partial v}{\partial y} \right)^2 &= -\frac{1}{\rho} \frac{\partial^2 p}{\partial y^2} + \nu \left(\frac{\partial^3 v}{\partial y \partial x^2} + \frac{\partial^3 v}{\partial y^3} \right),
\end{aligned}$$

and sum them together to obtain

$$\left(\frac{\partial u}{\partial x} \right)^2 + 2 \frac{\partial u}{\partial y} \frac{\partial v}{\partial x} + \left(\frac{\partial v}{\partial y} \right)^2 = -\frac{1}{\rho} \left(\frac{\partial^2 p}{\partial x^2} + \frac{\partial^2 p}{\partial y^2} \right),$$

where we have liberally used the incompressibility condition to simplify terms. Thus, we obtain three equations

$$\begin{aligned}
\frac{\partial u}{\partial t} + u \frac{\partial u}{\partial x} + v \frac{\partial u}{\partial y} &= -\frac{1}{\rho} \frac{\partial p}{\partial x} + \nu \left(\frac{\partial^2 u}{\partial x^2} + \frac{\partial^2 u}{\partial y^2} \right), \\
\frac{\partial v}{\partial t} + u \frac{\partial v}{\partial x} + v \frac{\partial v}{\partial y} &= -\frac{1}{\rho} \frac{\partial p}{\partial y} + \nu \left(\frac{\partial^2 v}{\partial x^2} + \frac{\partial^2 v}{\partial y^2} \right), \\
\left(\frac{\partial u}{\partial x} \right)^2 + 2 \frac{\partial u}{\partial y} \frac{\partial v}{\partial x} + \left(\frac{\partial v}{\partial y} \right)^2 &= -\frac{1}{\rho} \left(\frac{\partial^2 p}{\partial x^2} + \frac{\partial^2 p}{\partial y^2} \right),
\end{aligned}$$

which we may discretize using forward-difference, midpoint, and backward-difference

schemes

$$\begin{aligned} & \frac{u_{i,j}^{n+1} - u_{i,j}^n}{\Delta t} + u_{i,j}^n \frac{u_{i,j}^n - u_{i-1,j}^n}{\Delta x} + v_{i,j}^n \frac{u_{i,j}^n - u_{i,j-1}^n}{\Delta y} \\ &= -\frac{1}{\rho} \frac{p_{i+1,j}^n - p_{i-1,j}^n}{2 \Delta x} + v \left(\frac{u_{i+1,j}^n - 2u_{i,j}^n + u_{i-1,j}^n}{\Delta x^2} + \frac{u_{i,j+1}^n - 2u_{i,j}^n + u_{i,j-1}^n}{\Delta y^2} \right), \end{aligned}$$

$$\begin{aligned} & \frac{v_{i,j}^{n+1} - v_{i,j}^n}{\Delta t} + u_{i,j}^n \frac{v_{i,j}^n - v_{i-1,j}^n}{\Delta x} + v_{i,j}^n \frac{v_{i,j}^n - v_{i,j-1}^n}{\Delta y} \\ &= -\frac{1}{\rho} \frac{p_{i+1,j}^n - p_{i-1,j}^n}{2 \Delta x} + v \left(\frac{v_{i+1,j}^n - 2v_{i,j}^n + v_{i-1,j}^n}{\Delta x^2} + \frac{v_{i,j+1}^n - 2v_{i,j}^n + v_{i,j-1}^n}{\Delta y^2} \right), \end{aligned}$$

$$\begin{aligned} & \left(\frac{u_{i+1,j}^n - u_{i-1,j}^n}{2 \Delta x} \right)^2 + 2 \left(\frac{u_{i,j+1}^n - u_{i,j-1}^n}{2 \Delta y} \right) \left(\frac{v_{i+1,j}^n - v_{i-1,j}^n}{2 \Delta x} \right) + \left(\frac{v_{i,j+1}^n - v_{i,j-1}^n}{2 \Delta y} \right)^2 \\ &= -\frac{1}{\rho} \left(\frac{p_{i+1,j}^n - 2p_{i,j}^n + p_{i-1,j}^n}{\Delta x^2} + \frac{p_{i,j+1}^n - 2p_{i,j}^n + p_{i,j-1}^n}{\Delta y^2} \right) \end{aligned}$$

and rearrange to obtain

$$\begin{aligned} u_{i,j}^{n+1} = u_{i,j}^n + \Delta t \left(-\frac{1}{\rho} \frac{p_{i+1,j}^n - p_{i-1,j}^n}{2 \Delta x} + v \left(\frac{u_{i+1,j}^n - 2u_{i,j}^n + u_{i-1,j}^n}{\Delta x^2} + \frac{u_{i,j+1}^n - 2u_{i,j}^n + u_{i,j-1}^n}{\Delta y^2} \right) \right. \\ \left. - u_{i,j}^n \frac{u_{i,j}^n - u_{i-1,j}^n}{\Delta x} - v_{i,j}^n \frac{u_{i,j}^n - u_{i,j-1}^n}{\Delta y} \right), \end{aligned} \quad (3.7)$$

$$v_{i,j}^{n+1} = v_{i,j}^n + \Delta t \left(-\frac{1}{\rho} \frac{p_{i+1,j}^n - p_{i-1,j}^n}{2 \Delta x} + u \left(\frac{v_{i+1,j}^n - 2 v_{i,j}^n + v_{i-1,j}^n}{\Delta x^2} + \frac{v_{i,j+1}^n - 2 v_{i,j}^n + v_{i,j-1}^n}{\Delta y^2} \right) - u_{i,j}^n \frac{v_{i,j}^n - v_{i-1,j}^n}{\Delta x} - v_{i,j}^n \frac{v_{i,j}^n - v_{i,j-1}^n}{\Delta y} \right), \quad (3.8)$$

$$p_{i,j}^n = \frac{\Delta x^2 \Delta y^2 \rho}{2 (\Delta x + \Delta y)} \left[\left(\frac{u_{i+1,j}^n - u_{i-1,j}^n}{2 \Delta x} \right)^2 + 2 \left(\frac{u_{i,j+1}^n - u_{i,j-1}^n}{2 \Delta y} \right) \left(\frac{v_{i+1,j}^n - v_{i-1,j}^n}{2 \Delta x} \right) + \left(\frac{v_{i,j+1}^n - v_{i,j-1}^n}{2 \Delta y} \right)^2 - \frac{1}{2} \left(\frac{p_{i+1,j}^n + p_{i-1,j}^n}{\Delta x^2} + \frac{p_{i,j+1}^n + p_{i,j-1}^n}{\Delta y^2} \right) \right]. \quad (3.9)$$

We may now use Equations 3.7, 3.8, and 3.9 sequentially to approximate fluid flows in the following manner:

1. Have initial conditions based on the physical constraints of the system.
2. Iterate Equation 3.9 repeatedly to “smooth out” the pressure.
3. Use the “smoothed out” pressure in Equations 3.7 and 3.8 to approximate the fluid flow velocity at the next time step.
4. Use the approximated fluid flow velocity to repeat Step 2.

Section 3.4: Implementation Examples

In this section, we present several elementary fluid flows simulated in Python, including cavity flow and channel flow. For examples of code for such simulations, see [2].

Cavity Flow

Imagine blowing across the surface of your morning cup of coffee or tea to cool it down, or wind blowing across a small puddle. One would expect, as an effect of the no-slip condition,

that the surface would move at the same speed of the air, colliding with the opposite side of the container and creating an area of higher pressure. The fluid would then flow downward into the cavity, as the air is not moving fast enough to push it out of the container. The fluid would then cycle around, rising back to the surface to meet the air once more.

To simulate this system, we begin creating a cavity for our system, the range of spatial values we wish to simulate. For our purposes, we assume a square cavity with walls at $x = 0, 2$ and $y = 0$ in units of length, and the open “lid” at $y = 2$. We assume the moving air acts uniformly across this lid, such that $u = 1$ at $y = 2$. From the no-slip condition, we have $u, v = 0$ along the other boundaries. We must also account for boundary conditions for the pressure, for which we assume $\frac{\partial p}{\partial y} = 0$ at $y = 0$ and $\frac{\partial p}{\partial x} = 0$ at $x = 0, 2$.

Assuming this system will achieve a steady state under these constant conditions, we may assume $u, v, p = 0$ everywhere else and execute the simulation until the flow is sufficiently approximated, i.e., the difference in flow at each point between steps t_i and t_{i+1} is small (see Figure 3.3).

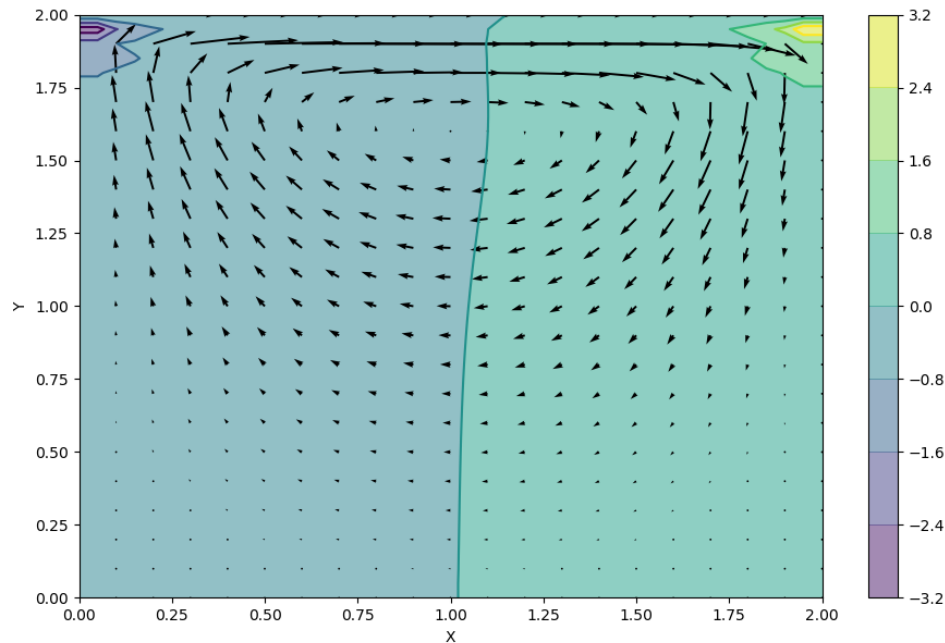


Figure 3.3: A cavity flow simulated in Python, where the flow is represented by the vector field and pressure by the contour plot in the background. See [2] for an example source code.

Channel Flow

We now consider a model for channel flow, such as that of water through plumbing or blood through veins and arteries. We again use a spatial grid between $x = 0, 2$ and $y = 0, 2$, where $y = 0, 2$ are rigid boundaries. Hence, we have $u, v, \frac{\partial p}{\partial y} = 0$ at these boundaries. To obtain a constant pressure gradient, we slightly modify Equation 3.7 to include an additional term F which we assign a value of 1,

$$u_{i,j}^{n+1} = u_{i,j}^n + \Delta t \left(-\frac{1}{\rho} \frac{p_{i+1,j}^n - p_{i-1,j}^n}{2 \Delta x} + v \left(\frac{u_{i+1,j}^n - 2u_{i,j}^n + u_{i-1,j}^n}{\Delta x^2} + \frac{u_{i,j+1}^n - 2u_{i,j}^n + u_{i,j-1}^n}{\Delta y^2} \right) - u_{i,j}^n \frac{u_{i,j}^n - u_{i-1,j}^n}{\Delta x} - v_{i,j}^n \frac{u_{i,j}^n - u_{i,j-1}^n}{\Delta y} \right) + F. \quad (3.10)$$

To simulate this flow, we require one additional tool: periodic boundary conditions. With periodic boundary conditions, we assume that our system is translationally symmetric, i.e., our system is unit cell in a perfect tiling (see Figure 3.4).

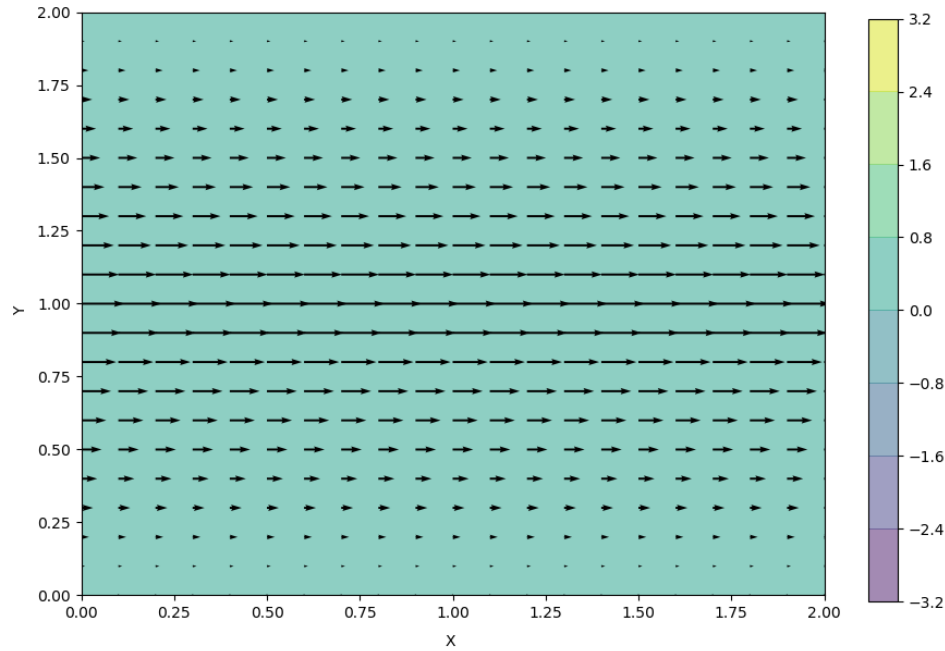


Figure 3.4: A channel flow simulated in Python, where the flow is represented by the vector field and pressure by the contour plot in the background. See [2] for an example source code.

Channel Flow with Blockage

We now insert a rectangular blockage into our channel, which may serve as a simple model of debris in pipes or plaque buildup in arteries. We extend our channel to $x = 0, 12$ and $y = 0, 4$, in order for the flow to at the end of the channel to become regular once more. Our blockage consists of a rectangle in the region $x = 4.2, 7.8$ and $y = 1.5, 2.5$. Throughout this region we have $u, v, p = 0$, while on the boundary of this region we apply the no-slip condition and the boundary conditions for the pressure.

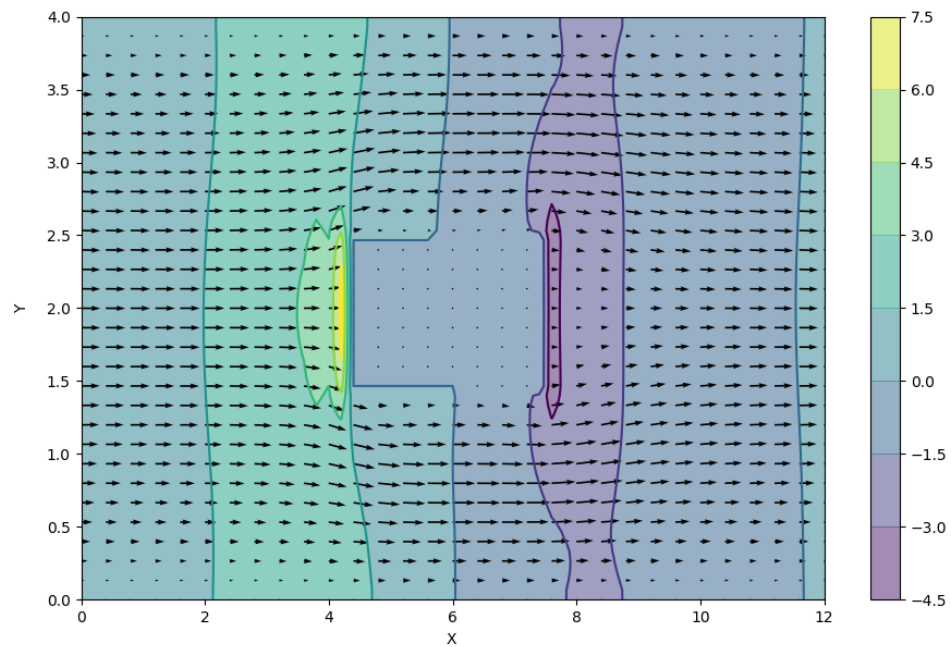


Figure 3.5: A channel flow with a blockage simulated in Python, where the flow is represented by the vector field and pressure by the contour plot in the background.

Bibliography

- [1] ACHESON, D. J. *Elementary Fluid Dynamics*. Oxford University Press, New York, 2005.
- [2] BARBA, L. A. 12 steps to navier-stokes. Electronic, 2013. Accessed March 2018 from <http://lorenabarba.com/blog/cfd-python-12-steps-to-navier-stokes/>.
- [3] FERZIGER, J. H., AND PERIĆ, M. *Computational Methods for Fluid Dynamics*. Springer, New York, 2002.
- [4] FITZPATRICK, R. *Theoretical Fluid Dynamics*. IOP Publishing, Bristol, UK, 2017.
- [5] KERSALÈ, E. Math2620: Fluid dynamics 1. 2017.